

Entropy as a measure of the performance of phosphor materials used in medical imaging radiation detectors

D. Cavouras^{1,*}, I. Kandarakis¹, T. Maris², G.S. Panayiotakis³, C.D. Nomicos⁴

¹Department of Medical Instrumentation Technology, TEI of Athens, Ag. Spyridonos Street, Aigaleo, 12210 Athens, Greece

²Department of Radiology, University Hospital, Medical School, University of Crete, Heraklion, Greece

³Department of Medical Physics, Medical School, University of Patras, 26500 Patras, Greece

⁴Department of Electronics, TEI of Athens, Ag. Spyridonos Street, Aigaleo, 12210 Athens, Greece

Received: 7 January 2000/Accepted: 28 March 2000/Published online: 23 August 2000 – © Springer-Verlag 2000

Abstract. In information theory, entropy expresses the information gain obtained after detection of a signal concerning the state of a parameter of interest. In this study, entropy has been expressed in terms of physical quantities (emitted optical fluence and MTF) related to the imaging performance of phosphor materials, which are employed in medical imaging radiation detectors. Four phosphor materials, used in the form of laboratory-prepared fluorescent layers (screens), were compared on the basis of their entropy performance. Measurements were performed using 30- and 80-kVp X-ray beams often employed in X-ray imaging. Results showed that phosphor materials with high density and effective atomic number exhibit high entropy performance, especially at the higher X-ray tube voltage of 80 kVp. Entropy values are also affected by the type of activator, which determines the intrinsic X-ray-to-light conversion efficiency, and the spectrum of emitted light. The proximity of the incident X-ray quanta energy to the energy of the K-shell threshold for photoelectric absorption is an additional important factor which increases entropy. This effect was more apparent in the performance of yttrium-based phosphors at the lower voltage of 30 kVp.

PACS: 78.65; 42.80.

Information theory has been developed since 1948 by Shannon and other workers [1, 2] in order to be applied in electrical and other types of communication systems. In the context of information theory, entropy is a parameter defined in order to quantify the amount of information provided to a receiver by a source. The name entropy, originating from statistical thermodynamics, has been adopted in this case, since it has been considered that information entropy is a measure of the disorder of the receiver's knowledge before detecting the information from the source [2]. Theory states that the information gain after receiving the signal corresponding to a certain value S of some physical quantity is given as $\log_2 1/p(S)$. $p(S)$ expresses the probability for a specific

value S to occur [2]. Entropy has been defined as the information gain averaged over all possible values of S by the formula:

$$H(S) = \int_0^{\infty} p(S) \log_2 \left[\frac{1}{p(S)} \right] dS = - \int_0^{\infty} p(S) \log_2 [p(S)] dS. \quad (1)$$

Since imaging systems may be considered as systems receiving, processing, and displaying information, information theory may be used to assess their performance. Previous studies have applied the concept of information capacity to evaluate radiographic and computed tomography systems [3, 4].

In the present study, entropy has been employed to assess the imaging performance of phosphors used in various types of medical imaging detectors (radiographic, fluoroscopic, digital imaging). Entropy has been expressed in terms of the following phosphor properties: (a) the emitted optical quantum fluence, (b) the X-ray-to-light conversion efficiency, (c) the efficiency to transmit light through a phosphor layer, and (d) the modulation transfer function (MTF), which expresses image contrast and spatial resolution. Four phosphor materials differing in their intrinsic physical properties (density, effective atomic number, activator, emission wavelength, and energy of the K-edge of photoelectric absorption) were examined. To our knowledge, entropy has not been previously used for assessing the imaging performance of phosphors.

1 Material and methods

Relation (1) expresses entropy as related to a continuously varying frequency-dependent parameter. As has been previously demonstrated [2], the information gain may be maximized if S is limited to a frequency bandwidth Δf , which includes both signal and noise which are additive, independent of each other, Gaussian and limited to an average signal power (P_S) and noise power (P_N). Then considering $p(S)$ as

*Corresponding author.

(Fax: +301/5910-975, E-mail: cavouras@hol.gr; cavouras@ee.teiath.gr)

a normal distribution function, it can be shown [2] that:

$$H(S) = \Delta f \log_2 [2\pi e\sigma^2] \quad (\text{in bits/s}), \quad (2)$$

where σ is the standard deviation of the distribution $p(S)$, which is equal to $\sigma^2 = \bar{S}^2 = P_S + P_N$. P_S and P_N must be invariant over the bandwidth Δf . If this is not the case and if P_S and P_N vary smoothly over Δf then integration over frequency may be performed [2] as follows:

$$H(S) = \int_0^{f_M} \log [2\pi e(P_S(f) + P_N(f))] df, \quad (3)$$

where f_M is the upper limit of the signal frequency bandwidth ($f_M - 0 = \Delta f$) and Δf is considered to be divided into small increments df , P_S and P_N being invariant within these increments.

In the case of medical images produced by phosphor layers, the mean output signal S_P may be expressed in the spatial frequency domain, using the concept of contrast transfer function ($\text{CTF}_P(f)$) [2, 5], as follows:

$$\bar{S}_P(f) = \bar{Q}_X \text{CTF}_P(f), \quad (4)$$

where \bar{Q}_X is the mean X-ray quantum fluence incident on the phosphor layer and the subscript P denotes the phosphor. The $\text{CTF}(f)$ of radiographic film screen systems has been expressed [5, 6] as the product of the slope of the characteristic curve (optical density versus log of relative exposure) and MTF. In the case of a phosphor layer, the slope of the characteristic curve may be expressed by the ratio $d\Phi_\lambda/dQ_X$, Φ_λ denoting the optical quantum fluence emitted by the excited phosphor. Hence,

$$\bar{S}_P(f) = \bar{Q}_X \left[\frac{d\bar{\Phi}_\lambda}{d\bar{Q}_X} \right] \text{MTF}_P(f), \quad (5)$$

and thus

$$\bar{S}_P(f) = \bar{\Phi}_\lambda \text{MTF}_P(f), \quad (6)$$

$\bar{\Phi}_\lambda$ being the mean emitted optical quantum fluence. The signal power spectrum $P_S(f)$ may then be written as

$$P_S(f) = [\bar{\Phi}_\lambda \text{MTF}_P(f)]^2. \quad (7)$$

The noise power spectrum has been expressed [7] by the relation:

$$P_N(f) = \bar{\Phi}_\lambda [\bar{m}_o(E)\bar{g}_L(\lambda)\text{MTF}_P^2(f)] + \bar{\Phi}_\lambda, \quad (8)$$

where $\bar{m}_o(E)$ is the average number of optical photons produced within the phosphor per X-ray quantum absorbed of mean energy E , $\bar{g}_L(\lambda)$ is the average light transmission efficiency of the phosphor expressing the probability of an optical quantum of wavelength λ to escape the phosphor [7–9]. It must be noted that $P_N(f)$ is the noise power spectrum associated with the optical quanta emitted by the phosphor, which is often called quantum noise power spectrum. Relation (8) does not account for the naturally present phosphor's fixed pattern noise. The latter should alter slightly the values of

$P_N(f)$ and $H(S)$. However as has been previously found, in a well-prepared phosphor screen, fixed pattern noise may be considered negligible [6, 10]. According to relations (6)–(8), entropy may be expressed as a function of phosphor material properties $\bar{\Phi}_\lambda$, \bar{m}_o , \bar{g}_L and MTF.

Explicitly:

- $\bar{\Phi}_\lambda$ is a function of: (i) the incident X-ray quantum fluence \bar{Q}_X , (ii) the X-ray absorption efficiency, which depends on material density, effective atomic number and X-ray quantum energy, (iii) the intrinsic X-ray-to-light conversion efficiency, which depends on the type of activator (i.e. Tb^{3+} in $\text{La}_2\text{O}_2\text{S:Tb}$), and (iv) the light transmission efficiency $\bar{g}_L(\lambda)$.
- \bar{m}_o is determined by the intrinsic X-ray-to-light conversion efficiency and by the energy of optical photons, which in turn is a function of the light wavelength.
- $\bar{g}_L(\lambda)$ depends on the phosphor thickness and on the optical absorption and scattering properties. The latter depend on the wavelength of light and the size of phosphor particles (for example phosphor grains in granular radiographic screens). Additionally, $\bar{g}_L(\lambda)$ is affected by the penetration depth of X-rays, which depends on the X-ray absorption efficiency.
- MTF depends on the thickness of a phosphor layer and on the intrinsic optical scattering and absorption properties of the material.

Four phosphor materials $\text{La}_2\text{O}_2\text{S:Tb}$, $\text{Y}_2\text{O}_2\text{S:Tb}$, $\text{Y}_2\text{O}_2\text{S:Eu}$, $\text{Y}_2\text{O}_3\text{:Eu}$, were employed in the form of layers (or screens) of various coating weights ranging from approximately 30 to 182 mg/cm². The layers were prepared in laboratory from commercially supplied phosphor powders using a sedimentation technique [8, 9, 11–13]. The powders consisted of phosphor grains of 7 μm approximate mean size. Thus, layers prepared in this way are similar to granular screens used in a great variety of imaging applications such as conventional radiographic cassettes, digital radiography detectors, image intensifiers, portal imaging devices etc.

To experimentally determine the emitted optical fluence $\bar{\Phi}_\lambda$, the layers were irradiated with X-rays at 30 and 80 kVp. The emitted light was measured by a photomultiplier (EMI 9558 QB) coupled to an electrometer (Cary 401), as is explicitly described in previous studies [8, 9, 11–13]. The product $\bar{m}_o \cdot \bar{g}_L$ was determined by considering it equal to the number of optical quanta emitted per absorbed X-ray. Thus, $\bar{m}_o \cdot \bar{g}_L$, may be given by the relation:

$$\frac{\bar{\Phi}_\lambda}{\bar{Q}_X^{\text{ab}}} = \bar{m}_o \cdot \bar{g}_L, \quad (9)$$

where, \bar{Q}_X^{ab} is the mean absorbed fraction of incident X-ray quanta \bar{Q}_X . This fraction was determined by first determining \bar{Q}_X from exposure measurements [9, 11–15] and then multiplying by the phosphor X-ray absorption efficiency. The latter was calculated by considering that absorption follows an exponential law. The X-ray absorption coefficient for each phosphor was determined from data on chemical elements La, Y, O, S given by Storm and Israel [16, 17].

MTF was determined by performing measurements according to the square-wave response function (SWRF) method [9, 12, 18]. SWRF was first measured using a suitable test pattern (type-53 of Nuclear Associates), comprising

lead line pairs with spatial frequencies ranging from 0.25 to 10 lp/mm. This pattern was imaged on an X-ray film, which was illuminated by the light of the X-ray-excited phosphor layer. The film was placed in contact with the phosphor's emitting surface while the test pattern was placed on the irradiated phosphor side. The pattern images (SWRF) were digitized on a Microtec Scanmaker II SP (1200 × 1200 dpi) scanner. The MTF was then determined using the digitized SWRF values and Coltman's formula [9, 12, 18]:

$$\text{MTF}_P(f) = \frac{4}{\pi} \sum_{k=1}^{\infty} b_K \frac{\text{SWRF}[(2k-1)f]}{(2k-1)}, \quad (10)$$

for $k = 1, 3, 5, \dots$,

where

$$b_K = 0, \quad \text{for } m < n, \\ b_K = (-1)^n (-1)^{k-1}, \quad \text{for } m = n. \quad (11)$$

n is the number of prime factors other than unity in $(2k-1)$, m is the number of prime factors other than unity which appear only once in $(2k-1)$.

To obtain the phosphor MTF, the values obtained by relation (10) were divided by the scanner and film MTFs, which were determined by the same method. The upper frequency limit, f_M in relation (3), was selected equal to 100 cycles/cm.

2 Results and discussion

Figure 1 shows the variation of the emitted optical quantum fluence with coating weight for $\text{La}_2\text{O}_2\text{S:Tb}$, $\text{Y}_2\text{O}_2\text{S:Tb}$, $\text{Y}_2\text{O}_2\text{S:Eu}$, $\text{Y}_2\text{O}_3\text{:Eu}$ phosphors measured at 80 kVp (corresponding to 1.12×10^4 quanta/mm²). $\text{La}_2\text{O}_2\text{S:Tb}$ was found to have the highest performance with respect to the other materials. Highest fluence values were obtained for the 82-

and 104-mg/cm² layers. The shape of the $\text{Y}_2\text{O}_2\text{S:Tb}$ optical quantum fluence curve was very similar to that of $\text{La}_2\text{O}_2\text{S:Tb}$ but with significantly lower values. $\text{Y}_2\text{O}_3\text{:Eu}$ was found with the lowest of the optical quantum fluence values. The shape of the curves is due to the combined effects [17] of: (i) the X-ray absorption efficiency, which increases exponentially with phosphor thickness and (ii) the light transmission efficiency, which decreases at thick phosphor layers, since optical quanta travel long distances to escape the phosphor and, hence, the probability of light attenuation is augmented. Thus, X-ray absorption initially increases rapidly with thickness, causing a similar increase in the emitted optical quantum fluence. As the phosphor thickness increases, X-ray absorption tends towards a saturation value. For higher coating weights, the decrease of light transmission efficiency becomes more dominant, resulting in reduced emitted optical quantum fluence. $\text{La}_2\text{O}_2\text{S:Tb}$ is the phosphor with the highest density and effective atomic number and consequently it exhibits highest X-ray absorption and emitted optical quantum fluence. Yttrium-based phosphors have lower density and effective atomic number resulting in lower X-ray absorption and light emission performance. Differences in both the shape and optical fluence values between $\text{Y}_2\text{O}_2\text{S:Tb}$ and $\text{Y}_2\text{O}_2\text{S:Eu}$ are due to the different ion activators (Tb^{3+} , Eu^{3+}), which affect the intrinsic conversion efficiency and the light emission spectrum. $\text{Y}_2\text{O}_2\text{S:Eu}$ has lower intrinsic efficiency (0.11) [19] than $\text{Y}_2\text{O}_2\text{S:Tb}$ (0.18) and this explains the lower Φ_λ values of $\text{Y}_2\text{O}_2\text{S:Eu}$ at low coating weights. On the other hand, $\text{Y}_2\text{O}_2\text{S:Eu}$ emits reddish light, which exhibits lower light attenuation coefficients (absorption-scattering) than the greenish light of $\text{Y}_2\text{O}_2\text{S:Tb}$. Thus, optical quanta produced within $\text{Y}_2\text{O}_2\text{S:Eu}$ are more penetrating and this explains the relative high Φ_λ values and the different curve shape at high coating weights.

Figure 2 shows the emitted optical quantum fluence of the four phosphor materials measured at 30 kVp. $\text{Y}_2\text{O}_2\text{S:Tb}$ was found superior to $\text{La}_2\text{O}_2\text{S:Tb}$ for coating weights up to

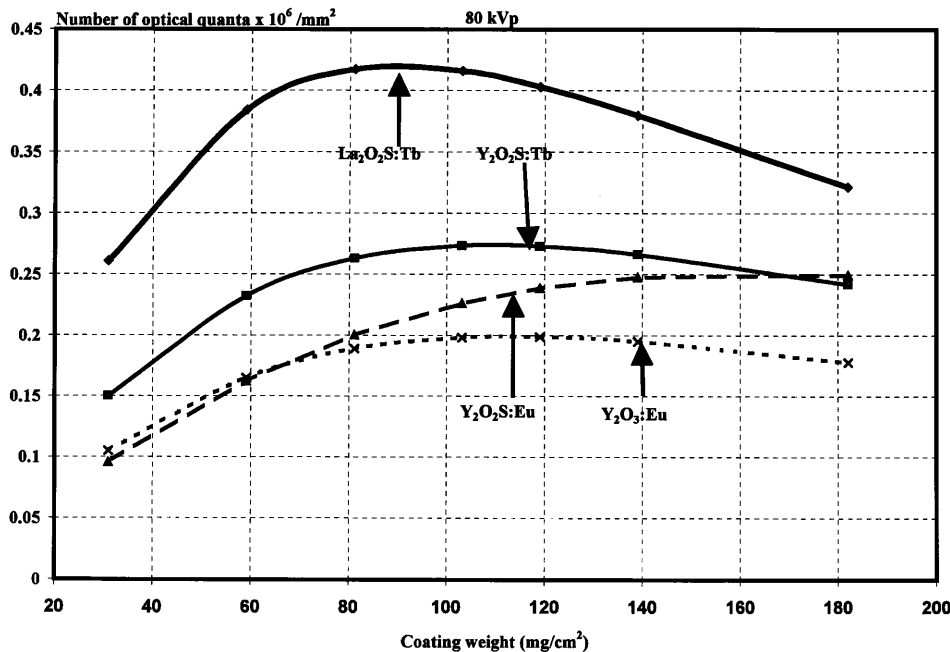


Fig. 1. Variation of emitted optical quantum fluence with coating weight for $\text{La}_2\text{O}_2\text{S:Tb}$, $\text{Y}_2\text{O}_2\text{S:Tb}$, $\text{Y}_2\text{O}_2\text{S:Eu}$, $\text{Y}_2\text{O}_3\text{:Eu}$ phosphors measured at 80 kVp

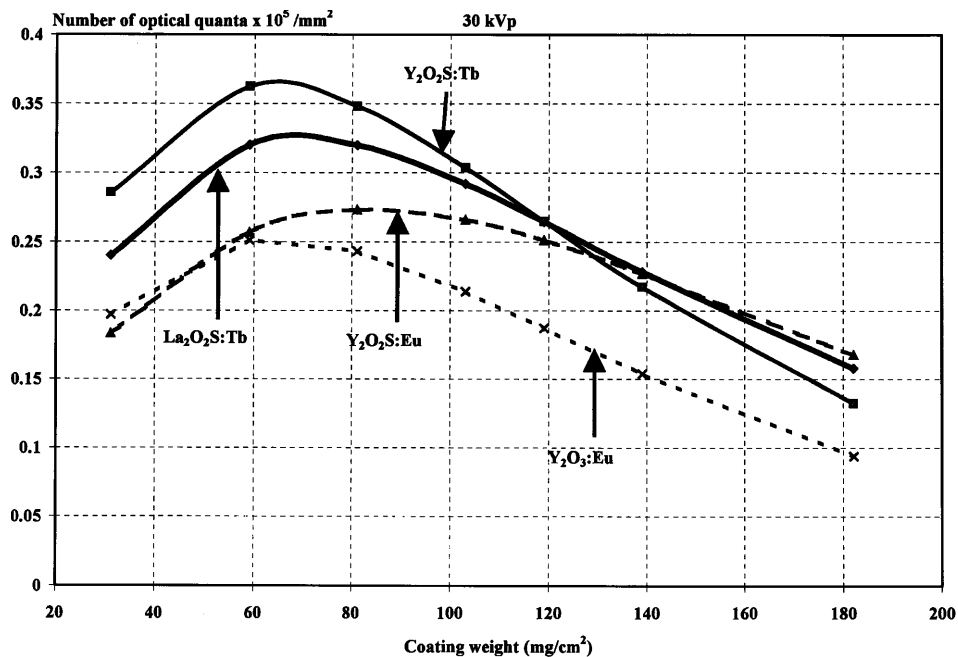


Fig. 2. Variation of emitted optical quantum fluence with coating weight for $\text{La}_2\text{O}_2\text{S:Tb}$, $\text{Y}_2\text{O}_2\text{S:Tb}$, $\text{Y}_2\text{O}_2\text{S:Eu}$, $\text{Y}_2\text{O}_3:\text{Eu}$ phosphors measured at 30 kVp

120 mg/cm^2 . This result may be explained by considering that, at 30 kVp, the mean energy of X-ray quanta is very close to the energy of the K-absorption edge of yttrium for the photoelectric effect, which lies at 17 keV. This increases both X-ray absorption efficiency and, hence, emitted optical quantum fluence of $\text{Y}_2\text{O}_2\text{S:Tb}$. At coating weights higher than 140 mg/cm^2 $\text{Y}_2\text{O}_2\text{S:Eu}$ showed highest performance slightly exceeding the performance of $\text{La}_2\text{O}_2\text{S:Tb}$. This is because of the lower light attenuation coefficients of $\text{Y}_2\text{O}_2\text{S:Eu}$ affected by the lower frequency of the emitted light.

Figure 3 shows the MTF as a function of spatial frequency for the four phosphor materials, measured at 80 kVp for layers of approximately 81 mg/cm^2 coating weight. The MTF of the digitizing scanner is also plotted. $\text{La}_2\text{O}_2\text{S:Tb}$ was found with the highest and $\text{Y}_2\text{O}_3:\text{Eu}$ with the lowest MTF

values. The superiority of $\text{La}_2\text{O}_2\text{S:Tb}$ may be explained by considering the higher density of this material. High density imposes that for equal phosphor coating weight, the thickness (in μm) of the phosphor layer will be thinner than the layer from a lower-density material. However, the amount of light spread, which degrades spatial resolution and MTF, is diminished within thin layers. This is because, when the layer is thin, both laterally directed and scattered optical quanta travel shorter distances to arrive at the phosphor's emitting surface. As a result the area over which the light spreads is restricted, thus improving spatial resolution and MTF. Similar reasoning may be applied to data obtained at 30 kVp, not shown since they were very similar to those of Fig. 3.

Figure 4 shows the variation of MTF with spatial frequency for seven $\text{La}_2\text{O}_2\text{S:Tb}$ phosphor layers of different

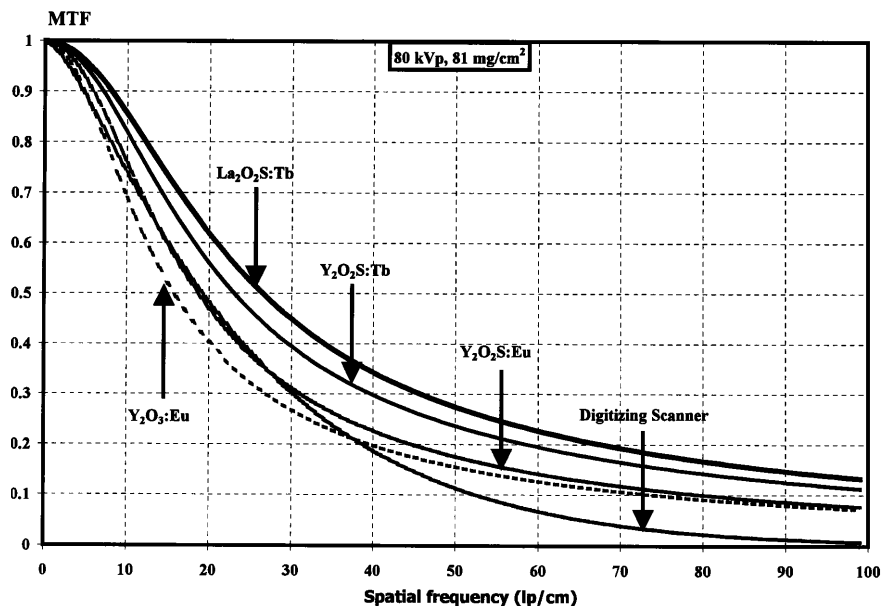


Fig. 3. MTF of $\text{La}_2\text{O}_2\text{S:Tb}$, $\text{Y}_2\text{O}_2\text{S:Tb}$, $\text{Y}_2\text{O}_2\text{S:Eu}$, $\text{Y}_2\text{O}_3:\text{Eu}$ phosphors measured at 80 kVp and the MTF of the digitizing scanner

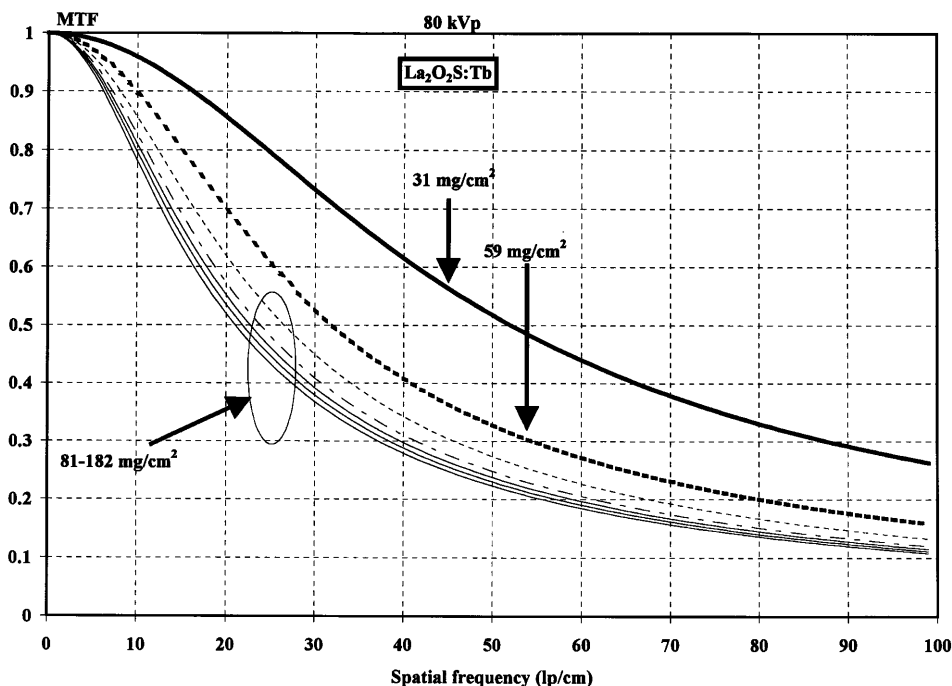


Fig. 4. Variation of MTF with spatial frequency for seven $\text{La}_2\text{O}_2\text{S:Tb}$ phosphor layers of different coating weight determined at 80 kVp

coating weight determined at 80 kVp. MTF decreases rapidly with coating weight up to 81 mg/cm^2 and thereafter MTF remains practically constant. This is because light spread increases with phosphor coating thickness. However at very thick layers the laterally directed optical quanta travel very long distances and, thus, the probability of their absorption within the phosphor is augmented. As a result their contribution to light spread is minimal and MTF remains unaltered.

Figure 5 shows the variation of entropy with phosphor coating weight, determined for the four phosphor materials at 80 kVp. Entropy curves showed a peak value at 30 mg/cm^2 and then entropy decreased continuously with increasing

phosphor layer thickness. This type of variation results from the combined effects of (i) the optical fluence emission (Φ_λ), which in most cases showed a maximum value at a certain coating weight but decreased thereafter (Figs. 1 and 2), and (ii) the image quality degradation, as expressed by the MTF decrease with phosphor thickness, due to light spread effects. As is shown in Fig. 4, MTF decreases very rapidly at the low coating weight range (up to 80 mg/cm^2) and this seems to reduce the effect of the initial increase of Φ_λ in the same range. $\text{La}_2\text{O}_2\text{S:Tb}$ was found to exhibit clearly higher entropy values than the other materials in the whole coating weight range. Additionally, $\text{Y}_2\text{O}_2\text{S:Tb}$ was also clearly better than $\text{Y}_2\text{O}_2\text{S:Eu}$ whereas $\text{Y}_2\text{O}_3\text{:Eu}$ which is characterized by

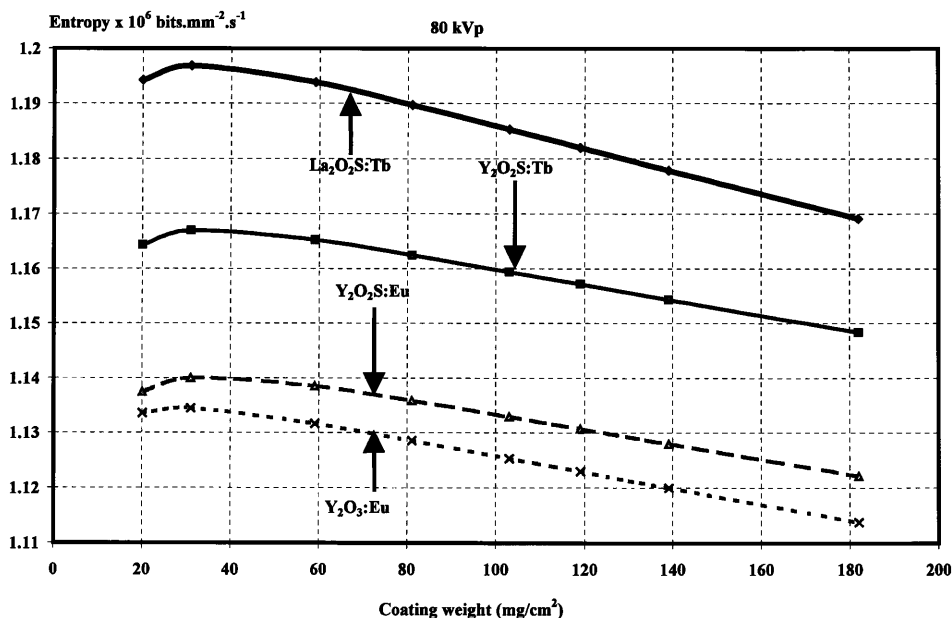


Fig. 5. Variation of entropy with phosphor coating weight for $\text{La}_2\text{O}_2\text{S:Tb}$, $\text{Y}_2\text{O}_2\text{S:Tb}$, $\text{Y}_2\text{O}_2\text{S:Eu}$, $\text{Y}_2\text{O}_3\text{:Eu}$ phosphors measured at 80 kVp

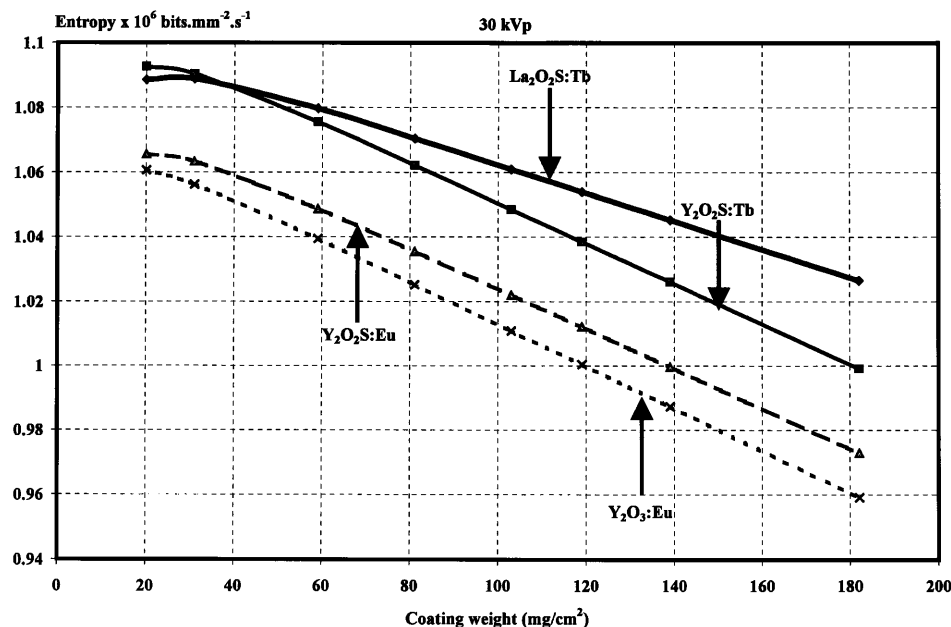


Fig. 6. Variation of entropy with phosphor coating weight for $\text{La}_2\text{O}_2\text{S:Tb}$, $\text{Y}_2\text{O}_2\text{S:Tb}$, $\text{Y}_2\text{O}_2\text{S:Eu}$, $\text{Y}_2\text{O}_3\text{:Eu}$ phosphors measured at 30 kVp

lowest density and effective atomic number, exhibited lowest entropy values.

In Fig. 6, entropy results obtained at 30 kVp showed an improvement of $\text{Y}_2\text{O}_2\text{S:Tb}$ with respect to $\text{La}_2\text{O}_2\text{S:Tb}$. For the 30-mg/cm² layers, $\text{Y}_2\text{O}_2\text{S:Tb}$ was found with slightly higher entropy than $\text{La}_2\text{O}_2\text{S:Tb}$. This improvement is explained by the increased X-ray absorption and light emission of yttrium phosphors at X-ray energies in the proximity of their K-absorption edge at 17 keV. These results are interesting for mammographic applications, where rather low X-ray tube voltages are employed. On the other hand, the data of Fig. 5 show that at higher voltages (80 kVp), mostly used in general radiography, materials with heavier atoms, such as La, are clearly more appropriate than yttrium-based phosphors. It is obvious that entropy, as applied to phosphor material performance, is strongly affected by the intrinsic properties of materials such as density, atomic number, activator type, light wavelength, and K-edge energy for photoelectric X-ray absorption. The combined effects of all these properties determine the variation of entropy with phosphor coating thickness and X-ray energy.

3 Conclusion

In this study it has been shown that, in the case of phosphor materials, information entropy may be related to image brightness (emitted optical fluence) and to image detail visibility (MTF). Thus, entropy may be employed for assessing the performance of phosphors for use in medical imaging detectors.

Acknowledgements. This study is dedicated to the memory of Prof. G.E. Giakoumakis, leading member of our team, whose work on phosphor materials has inspired us to continue.

References

1. C.E. Shannon: *Bell. Syst. Tech. J.* **27**, 379 (1948)
2. J.C. Dainty, R. Shaw: *Image Science* (Academic Press, London 1974)
3. H. Kanamori, M. Matsuoto: *Phys. Med. Biol.* **29**, 303 (1984)
4. R.F. Wagner, D.G. Brown, M.S. Paster: *Med. Phys.* **6**, 83 (1979)
5. R. Van Metter: *Med. Phys.* **19**, 53 (1992)
6. P.C. Bunch, K.E. Huff, R. Van Metter: *J. Opt. Soc. Am. A* **4**, 902 (1987)
7. R. Shaw, R. Van Metter: *Proc. SPIE* **454**, 128 (1984)
8. I. Kandarakis, D. Cavouras, P. Prassopoulos, E. Kanellopoulos, C.D. Nomicos, G.S. Panayiotakis: *Appl. Phys. A* **67**, 521 (1998)
9. I. Kandarakis, D. Cavouras, G.S. Panayiotakis, D. Triantis, C.D. Nomicos: *Nucl. Instr. Methods Phys. Res., Sect. A* **399**, 335 (1997)
10. G.T. Barnes: *Am. J. Roentgenol.* **127**, 189 (1976)
11. D. Cavouras, I. Kandarakis, A. Bakas, D. Triantis, C.D. Nomicos, G.S. Panayiotakis: *Br. J. Radiol.* **71**, 766 (1998)
12. D. Cavouras, I. Kandarakis, G.S. Panayiotakis, E.K. Evangelou, C.D. Nomicos: *Med. Phys.* **23**, 1965 (1996)
13. I. Kandarakis, D. Cavouras, E. Kanellopoulos, C.D. Nomicos, G.S. Panayiotakis: *Med. Biol. Eng. Comput.* **37**, 25 (1999)
14. J.R. Greening: *Fundamentals of Radiation Dosimetry*, in *Medical Physics Handbooks* (Institute of Physics, London 1985)
15. W.R. Hendee: *Medical Radiation Physics Year Book* (Medical Publishers, Chicago 1970)
16. E. Storm, H. Israel: Report LA-3753. (Los Alamos Scientific Laboratory of the University of California 1967)
17. G.W. Ludwig: *J. Electrochem. Soc.* **118**, 1152 (1971)
18. ICRU, Modulation transfer function of screen-film systems, ICRU Report 41, 1986
19. D. Cavouras, I. Kandarakis, G. Panayiotakis, E. Kanellopoulos, D. Triantis, C. Nomicos: *Appl. Rad. Isot.* **49**, 931 (1998)